



Supercritical carbonation of calcareous composites: Influence of curing



Elham Farahi^{a,1}, Phil Purnell^{b,*}, Neil R. Short^c

^a School of Engineering, University of Warwick, Coventry CV4 7AL, UK²

^b Institute for Resilient Infrastructure, School of Civil Engineering, University of Leeds, Leeds LS2 9JT, UK

^c School of Engineering and Applied Science, Aston University, Birmingham B4 7ET, UK²

ARTICLE INFO

Article history:

Received 15 October 2012

Received in revised form 7 June 2013

Accepted 12 June 2013

Available online 25 June 2013

Keywords:

Super-critical carbonation

Mechanical processing

Lime

Cement

Flexural testing

Petrography

Curing

ABSTRACT

This paper reports the effect of curing on the susceptibility of cementitious composites to carbonation using supercritical carbon dioxide. Samples made using a compression moulding technique were cured in water before and/or after carbonation and the effect on porosity, microstructure, solid phase assemblage and flexural strength was determined. In terms of development of mechanical strength, no benefit was gained from any period of pre- or post-carbonation curing regime. Yet samples cured prior to carbonation underwent minimal chemical reaction between supercritical carbon dioxide and calcium hydroxide, unhydrated cement or C–S–H. Thus there was no correlation between chemical degree of reaction and strength development. The effects responsible for the marked strength gain in supercritically carbonated samples must involve subtle changes in the microstructure of the C–S–H gel, not simple pore filling by calcium carbonate as is often postulated.

© 2013 Elsevier Ltd. All rights reserved.

1. Introduction

The effect of scCO_2 on cementitious materials was first investigated by the oil industry in the context of deep well linings, but its use as a treatment to improve the properties of cement composites was initiated by Jones in late 1990s [1–3]. Supercritical carbonation (SCC) of cementitious composites is chemically similar to natural carbonation in that the carbon dioxide diffuses into the capillary pores of the cement paste and combines with water present in capillary pores, forming carbonic acid (H_2CO_3). This acid dissociates into carbonate (CO_3^{2-}) and hydrogen (H^+) ions which then react with the portlandite ($\text{Ca}(\text{OH})_2$) formed during hydration, cement hydrates, any unhydrated cement (mainly C_3S and C_2S), and residual sodium and potassium ions in the pore solution of the cement matrix. In calcareous composites, the binder is formed from a mixture of cement and/or other calcium-bearing additive materials such as slaked lime, fly ash, and steel slag. The latter of these also contain a certain amount of active silica. These are generally added to improve technical properties, or to reduce environmental impact and/or cost by partially replacing cement binder with cheaper, potentially ‘low energy’ materials. In most cases, sufficient

siliceous material is retained in the matrix such that the principal binding phase remains C–S–H gel (in contrast to pure lime mortars). The scCO_2 will also react with the calcium-bearing phases in these additive materials.

These reactions form calcium carbonate, hydrated silica (as a result of decalcification of C–S–H gel) and other minor products including sodium and potassium carbonates and hydrated alumina [4–8]. Compared to natural or ordinarily accelerated carbonation however, SCC is greatly accelerated, with complete carbonation of engineering-sized components being achieved in hours rather than years. This is mainly attributable to the significant rise of CO_2 solubility in the pore solution, and the relative ease with which high-density scCO_2 can penetrate and diffuse into the cement paste pore network [7,8]. As with natural carbonation, the process reduces the hydroxide concentrations in the pore solutions, lowering its alkalinity from $\text{pH} = 12.5$ – 13.5 in uncarbonated cement paste down to $\text{pH} \approx 9$ in the fully carbonated zone. The exact pH will depend on the HCO_3/CO_3 equilibria, which in turn will be controlled by both the degree of carbonation and amount of alkalis (NaOH , KOH) present [4,9,10].

The carbonation process also alters the microstructure of calcareous based composites [1,7,8,11–15]. The molecular volume of calcium carbonate (normally calcite) is 11.2% greater than that of calcium hydroxide. Thus the calcite precipitated within the hardened cement paste (hcp) matrix during carbonation (both indirectly from the decalcification of C–S–H gel and accelerated hydration/carbonation of residual unhydrated cement particles,

* Corresponding author. Tel.: +44 113 343 0370.

E-mail addresses: elham.farahi@amec.com (E. Farahi), p.purnell@leeds.ac.uk (P. Purnell).

¹ Present address: AMEC, 601 Faraday Street, Birchwood Park, Birchwood, Warrington WA3 6GN, UK. Tel.: +44 1925 675489.

² Formerly.

and directly from carbonation of the free calcium hydroxide dispersed through the hcp) fills up pores with small tightly packed crystals of calcite. This reduces the total pore volume, pore size and permeability of the composite [4,6,10] and also enhances the compressive and flexural strength [7,8,10,16,17]. Accordingly, much recent work has focussed on documenting the improvements in the microstructural, mechanical and durability properties of cementitious composites afforded by treatment with scCO_2 [6,10–15,18–20]. Some researchers have investigated combination of novel production methods with SCC with a view to enabling mass-production of high-value functional and/or structural SCC ceramic composites from a range of starting materials including cement, lime, various aggregates and waste materials (e.g. PFA, steel slag) [21,22]. Aggregate chemistry and grading, binder composition and aggregate-binder ratios were all found to have significant effects on the properties of SCC cementitious composites.

The work reported in this paper was focused on understanding the effect of conventional wet curing (as commonly used for pre-cast concrete components) on: the rate and extent of carbonation; the flexural strength; and the microstructure of supercritically carbonated specimens of cementitious composites. For the SCC-treated samples, the effect of two curing scenarios was examined; curing prior to and curing after SCC treatment. This was done to examine if any technical benefit could be gained from such curing either before or after specimens are exposed to scCO_2 . These specimens were compared with uncarbonated, conventionally cured samples analogous to those currently manufactured in industry. The effect of these combinations of SCC treatment and moist curing was investigated using X-ray diffraction (XRD), combined differential thermal analysis with thermo-gravimetric analysis (DTA/TG), thin section petrography (TSP), helium pycnometry and a 4-point flexural strength test method.

2. Experimental methods

2.1. Materials

All specimens were manufactured with an aggregate to binder ratio of 5:2. The binder was 1.5:0.5 ordinary Portland cement [C]: hydrated lime [L] by mass; aggregate [A] was 65:35 by mass of crushed limestone: silica sand. These combinations were found to be optimal in previous work [23] with regard to ease of mechanical processing, reliability of carbonation and development of strength. The lime (Buxton Lime, UK) used comprised of >96% Ca(OH)_2 as determined using X-ray fluorescence (XRF) and the remainder made up of CaCO_3 , CaO , SiO_2 and Mg(OH)_2 . The Portland cement (Tarmac, UK) comprised 65% CaO , 20.25% SiO_2 , 5.3% Al_2O_3 , 3.25% Fe_2O_3 and 3.3% SO_3 , as determined by XRF and the remainder made up of MgO and K_2O . The crushed limestone [CL] (Buxton Lime/Tarmac, UK) comprised 98% CaCO_3 with upper:lower 20 percentile particle size of 2.0:0.15 mm and pure silica sand [S] (Buxton Lime/Tarmac, UK) had upper:lower 20 percentile particle size of 0.5:0.15 mm).

2.2. Sample preparation

Green samples (i.e. fresh, uncured and uncarbonated specimens with only sufficient strength for handling purposes) were manufactured using a compression moulding technique combined with vacuum dewatering. A two-part perforated stainless steel tool (Fig. 1) was used to produce six trapezoidal specimens per sample (length: 170 mm, width: 22/34 mm, depth: 17 mm) in each operation, using 9 MPa of pressure for 1 min, preliminary work having established this as the optimum processing conditions [23]. Excess water squeezed out of the samples was removed with a vacuum pump connected via a manifold to the perforations in the tool. The tool was lined with filter paper to prevent egress of solid

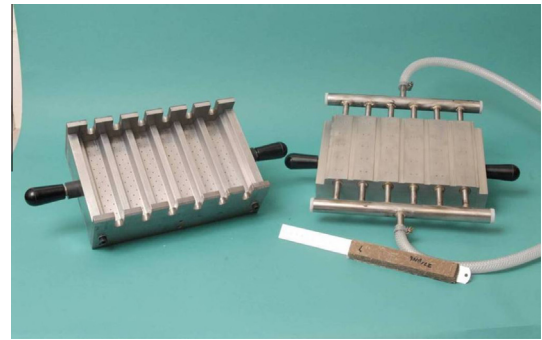


Fig. 1. Layout of the compression moulding tool.

material. Surplus samples were used to estimate the quantity of water removed during pressing. The water to binder ratio (w/c) of the cementitious paste within the 1.5C:0.5L:5A composite for the compression moulding process was 0.55. After pressing the w/c of manufactured green specimens was reduced to 0.3.

2.3. Wet curing and pre-conditioning and supercritical carbonation

Three distinct post-pressing treatment phases were used:

- Pre-conditioning: a partial drying treatment design to optimise moisture levels in the green specimens to promote carbonation [12,13,24]. Samples were dried in a fan oven for 12 h at 25 °C to remove ~75% of the free water.
- Curing: immersion in water at room temperature for 3, 7 or 28 days.
- SCC treatment: exposure to static water saturated scCO_2 at 60 °C, 10 MPa for 24 h in a sealed stainless steel pressure vessel (see Farahi et al. [22] for further details of the experimental set up). Corresponding control samples were stored sealed at room temperature during the 24 h period in which treated samples were undergoing SCC treatment.

These were combined in 7 sequences of experiments: 1 basic (C1), 2 pre-cured (C3, C7), 1 double-cured (C7-28) and 3 post-cured (C3*, C7*, C28*). Each sequence comprised a treated set exposed to SCC treatment, and a control set stored sealed at room temperature for 24 h. These are described below:

- C1: Preconditioning followed by either SCC treatment (treated) or stored sealed (control).
- C3: Curing for 3 days then preconditioning, followed by either SCC treatment (treated) or stored sealed (control).
- C7: as C3 but with 7 days of curing.
- C7-28: as C7 but followed by a further period of post-treatment curing for 28 days.
- C3*: as C1 but followed by post-treatment curing for 3 days.
- C7*: as C1 but followed by post-treatment curing for 7 days.
- C28*: as C1 but followed by post-treatment curing for 28 days.

At the end of each combination, samples were tested for mechanical and microstructural properties.

2.4. Mechanical testing

Triplicate specimens were tested for flexural strength using a fully articulated 4-point bending fixture attached to a screw controlled machine (Testometric Micro 100KN PCX). All testing was performed using a small load cell (100 kgf) and at a constant cross head displacement of 1 mm min^{-1} . Mid span deflection was measured using an integrated LVDT-type transducer. The machine

was controlled by computer software which captured all load–displacement data with 0.1 N and 1 μm resolution up to failure. Flexural strength at failure (modulus of rupture) was calculated using standard beam theory.

2.5. Chemical analysis

2.5.1. X-ray diffraction (XRD)

Immediately after mechanical testing, the degree of carbonation of treated specimens was analysed using XRD (Philips PW 1830). Small portions from each specimen were taken and finely ground to pass a 150 μm sieve. The analysis was then performed using Cu K α radiation between 15° and 80° 2 θ at 0.6° min^{−1} (0.02° per step, 2 s per step). For each scenario, triplicate control and carbonated specimens were tested and degree of carbonation was examined semi-quantitatively by computing the mean ratio of peak height of two most prominent peaks for portlandite (CH) and alite (C₃S) for the three control and three carbonated samples.

2.5.2. Thermal analysis

Combined differential thermal analysis/thermo-gravimetry (DTA/TG, PL-STA 1500), was used as a quantitative technique to determine the nature and relative concentrations of various compounds present in the samples such as calcium carbonate (C $\hat{\text{C}}$) and calcium hydroxide (CH). DTA-TG can also provide some information on the nature and relative quantity of compounds such as C–S–H gel that are amorphous and thus could not be recognised by XRD [25]. For this test, specimens were ground to pass a 150 μm sieve and then immediately analysed in air, between 20 and 1100 °C at a heating rate of 20 °C min^{−1}.

2.6. Helium pycnometry

Helium pycnometry was used to investigate the influence of the curing regimes and supercritical carbonation on the pore structure. For each case, 10 × 13 × 20 mm cuboids were cut from mechanical testing remnants using a precision saw and dried by immersion in acetone for 48 h, followed by storage over silica gel until reaching constant weight (taking between 14 and 21 days) after the method described by Aligizaki [26]. The cuboids were then accurately measured by micrometer and weighed, providing the bulk density. They were then tested in a helium pycnometer (AccuPyc 1330, Micromeritics) over 10 purge cycles to provide the true densities, from which the porosity was calculated. Samples were tested in triplicate.

2.7. Thin section petrography

Thin section petrography (TSP) was used to investigate the effect of mix design, curing and SCC on microstructure. TSP is a more useful method for examining the microstructure of a composite than SEM when authoritative identification of phases (eg differentiation between CH and C $\hat{\text{C}}$) is required [12,26]. Standard 30 μm thick, clear resin impregnated thin sections were prepared. The slides were then examined under a modified Vickers petrological microscope, using plane polarised, dark field plane polarised and/or crossed polarised light.

3. Results

3.1. Bending strength evaluation

Fig. 2 shows the variation in flexural strength of control vs. scCO₂ treated samples with curing conditions. As expected, SCC treatment results in a significant improvement in strength over

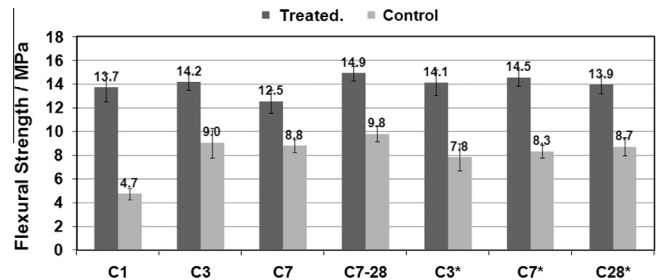


Fig. 2. Flexural strength vs. curing regime. Error bars = \pm st. dev.

control samples in all cases. However, no significant further benefit could be gained from any period of water curing prior to carbonation; only slight strength improvements were observed in specimens cured after carbonation. Thus, from a practical point of view, carbonation immediately after demoulding and pre-conditioning would be the preferred production option. The flexural strength of samples thus treated (C1, 13.7 MPa) was about 60% higher than that achieved by normal 28 days conventional curing (C28* control, 8.7 MPa).

3.2. XRD

XRD results (Figs. 3 and 4) showed complete depletion of crystalline CH and C₃S in samples carbonated immediately after pre-conditioning (C1, C3*, C7*, C28*), suggesting that treated samples were fully carbonated. For treated samples only wet-cured after carbonation (C3*, C7*, C28*), CH did not reappear in samples after they were exposed to water, suggesting that no amorphous C₃S (which would not be detected by XRD) is left after SCC treatment that can enable secondary hydration.

However, treated samples wet-cured before SCC treatment (C3, C7, C7-28) were resistant to carbonation and failed to become fully carbonated; significant amounts of CH and C₃S were detected in the samples after SCC treatment. More CH and C₃S remained in

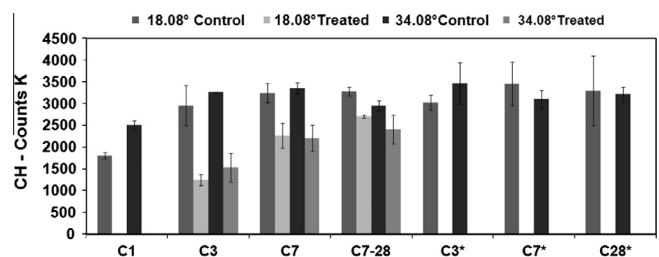


Fig. 3. XRD analysis of CH depletion vs. curing. Angles refer to 2 θ peaks on XRD traces using Cu K α radiation wavelength 1.5418 Å. Average of triplicate samples. Error bars = \pm 1 st. dev.

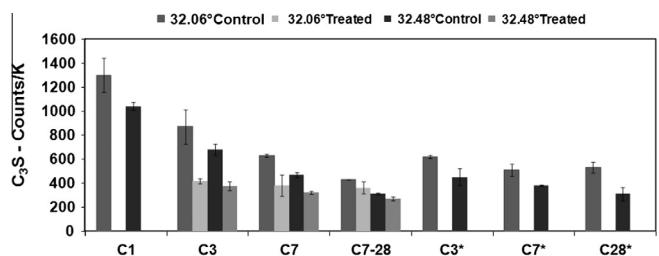


Fig. 4. XRD analysis of C₃S depletion vs. curing. Angles refer to 2 θ peaks on XRD traces using Cu K α radiation wavelength 1.5418 Å. Average of triplicate samples. Error bars = \pm 1 st. dev.

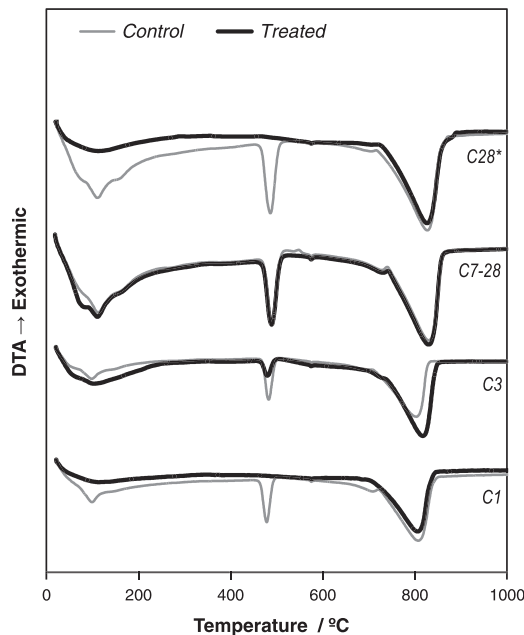


Fig. 5. DTA thermograms for control and treated samples cured under C1, C3, C7–28, C28* wet curing condition. Black line: treated samples. Gray line: control samples.

treated samples (compared to relevant control sample) exposed to longer curing prior to carbonation; in samples cured for 3 and 7 days prior to carbonation (C3, C7) CH and C₃S were depleted by 53% or 35–40% respectively by SCC treatment.

In samples exposed to both pre- and post-treatment curing (C7–28), the C₃S remaining after SCC treatment appeared to have its ability to further hydrate restricted, since the proportion of remaining C₃S further hydrated during post-treatment curing was much smaller for carbonated samples cf. control samples. Interestingly, the strength of treated C7–28 samples was the highest recorded (14.9 MPa) yet the degree of carbonation (as measured by CH and/or C₃S depletion) was lowest. These results confirm that traditional measurements of degree of carbonation (e.g. phenolphthalein indicator tests) are unlikely to be a useful guide to strength gains – and hence microstructural development – in carbonated samples; the rarely measured effect of carbonation on the gel phases (i.e. C–S–H) is likely to be much more important.

The amount of C₃S present in control samples was reduced as curing times increased, as expected.

3.3. DTA/TG

DTA/TG was used primarily to investigate samples cured prior to carbonation, in order to investigate the source of strength enhancement despite incomplete carbonation of crystalline

phases. Fig. 5 shows the DTA thermograms for C1, C3, C7–28 and C28*.

The endotherms between 100 and 200 °C reflect the dehydration of ‘low temperature hydrates’ (LTH) i.e. C–S–H gel and AF_t phases. For control samples, the area and complexity of the LTH peak increases with curing time as expected, reflecting continued hydration of the cement. The effect of SCC treatment on the LTH peak is markedly different depending on the curing sequence. For samples not exposed to pre-treatment curing, SCC treatment (C1, C28*) almost removes the LTH peak, suggesting that the gel phases are significantly affected (probably by decalcification and dehydration to form a silica gel). In contrast, for samples cured before treatment (C3, C7–28), the effect of SCC treatment on the LTH peak is much less marked and lessens with increased curing time; for C3, some broadening of the LTH peak can be observed but for C7–28 the peak remains essentially unchanged, retaining its sharpness and shoulders.

The endotherm between 450 and 530 °C is due to the dehydration of CH. In the cases where specimens were carbonated immediately after manufacturing (C1, C28*) CH has been depleted fully by the treatment. In the treated samples exposed to curing prior to carbonation (C3 and especially C7–28) a considerable amount of CH remained in the samples after SCC treatment; the longer they remained in water (C7–28 cf. C3), the more resistant they have become to carbonation of CH. These results confirm the XRD studies (Fig. 3).

The small blip at ~580 °C is caused by the $\alpha \rightarrow \beta$ crystal form inversion in the quartz sand aggregate [12].

The effects in the DTA thermograms at 650 °C onward are related to decomposition of calcium carbonate (CC). The contribution to these effects from the aggregate (65% limestone) tends to obscure those associated with development of CC from carbonation of CH, C₃S and C–S–H and thus no firm conclusion can be drawn. In this regard; quantitative TG analysis is required and this is shown in Table 1 (details of the calculations are given as a footnote to the table). The analysis confirmed a significant increase in CC content in samples not cured before SCC treatment (C1, C28*), but little or no calcite development in those cured before SCC treatment (C2, C7–28). TG analysis also confirmed that a significant amount of CH remained in samples cured before SCC treatment (C3, C7–28) while samples exposed immediately to scCO₂ (C1 and C28*), CH was shown to be removed completely, confirming the results of the XRD study. For the C3 samples, the degree of CH depletion according to XRD (~50%) was somewhat less than that measured using TG (~70%), suggesting that amorphous CH present in the hcp carbonated preferentially. As with the XRD analysis, strength development was not necessarily correlated with degree of carbonation.

3.4. Porosity measurement

Helium pycnometry was carried out the same sample subset as DTA/TG (C1, C3, C7–28 and C28*). Results (Fig. 6) suggested that in

Table 1

Quantitative analysis of TG traces for treated and control samples exposed to following curing regimes. Samples made from; 1.5C:0.5L:5A (A = 65:56 CL:S).

'Wet' curing regimes	LTH (%)		Ca(OH) (% w/w)		CaCO ₃ (% w/w)	
	Treated	Control	Treated	Control	Treated	Control
C1	1	1.59	0	4.73	57.59	47.4
C3	2.44	2.39	1.64	5.43	50.98	48.76
C7–28	3.63	3.52	5.75	6.99	45.04	45.04
C28*	1.29	3.41	0	6.99	57.84	47.15

LTH (%): mass loss (%) recorded between 20 and 200 °C. Note: no correction for background drift.

Ca(OH)₂ (%): CH content determined from the mass loss on TG traces between 450 and 530 °C. Note: corrected for background drift.

CaCO₃ (%): calcite content determined by the mass loss on TG traces between 650 and 875 °C. Note: corrected for background drift.

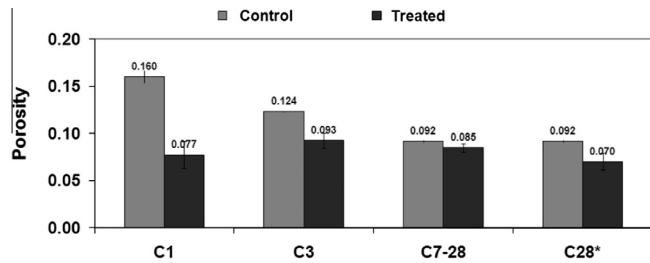


Fig. 6. Porosity measurements by Helium pycnometry for mix design 1.5C:0.5L:5A vs. Curing regimes. Treated = 60 °C, 100 bar, 24 h. A = 65:56 CL:S. All proportions w:w. Error bars = \pm st. dev.

all cases, the total porosity of the composite was reduced to 0.08 ± 0.01 by the SCC treatment, which would partially account for the increase in strength observed. However, for samples with well-developed pre-treatment microstructure (i.e. C7-28), relatively small changes in porosity (-8%) lead to large increases in strength ($+34\%$); also, where untreated and SCC treated samples have very similar porosity (C28* control and/or C7-28 control, cf. C3 treated), the SCC treated sample has much higher strength (9 – 10 MPa, cf. 14.2 MPa respectively, see Fig. 2). This suggests that the strength enhancement effect of SCC treatment is more profound than a simple reduction in porosity; the intrinsic strength of the matrix is also significantly increased.

Increased degree of water curing decreased the porosity of control samples, as expected.

3.5. Petrography

Fig. 7 shows the microstructure of an uncarbonated, minimally cured (C1 control) sample. Typical limestone (L) and sand (i.e. quartz, Q) particles have been marked. The groundmass – the material between distinct particles – is generally dark, owing to the poorly crystalline residual unhydrated cement minerals and some CSH gel, studded with bright flecks of small calcium hydroxide crystals and the occasional larger CH crystal (marked CH). The interface between the aggregate particles and the groundmass is not intimate and some porosity can be observed. Since the control sample is uncured and unhydrated, the space at aggregate/matrix interface is largely free of hydration products.

In carbonated samples (Fig. 8, C1 treated) however, the groundmass is much lighter and featureless, composed of cryptocrystalline calcium carbonate (identifiable by its high birefringence) mixed with an amorphous phase, presumably decalcified CSH gel. The dark inclusions are pseudomorphs of unhydrated cement

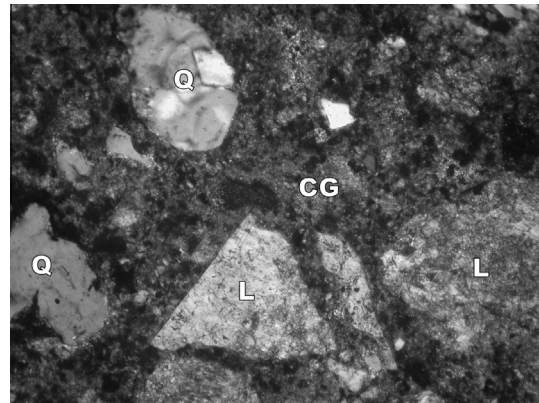


Fig. 8. Thin section micrograph (TSM) of C1 scCO₂-treated sample. Horizontal field of view = 0.7 mm.

grains, which have been carbonated. Compared to control samples, the porosity within the groundmass has reduced considerably, correlating with the helium pycnometry results. There is also very little porosity at the interface between aggregate particles and groundmass; the interface between the limestone and the carbonated groundmass (CG) is now quite indistinct in places.

Fig. 9 shows the microstructure of a C7-28 SCC-treated sample (note the change of scale); the section was taken to include sample surface exposed to scCO₂, which can be seen at the bottom of the figure. The penetration and reaction of the scCO₂ has clearly been impeded by the pre-cured microstructure; only a relatively shallow (~ 0.5 mm) layer near the surface has fully carbonated groundmass (CG), while deeper in the sample it remains largely uncarbonated (UG).

4. Discussion and conclusions

The results from the flexural testing clearly demonstrate that from the point of view of developing mechanical strength, there is no benefit in any period of pre- and/or post-treatment curing. SCC treatment immediately after pressing and pre-conditioning imbues strength well above that which could be expected to be developed by curing alone, and does so within hours rather than days.

Nonetheless, the pre-curing experiments have uncovered an interesting phenomenon; namely that there is almost no correlation between the 'degree of carbonation' – i.e. the extent to which CH, residual unhydrated cement and C–S–H gel have reacted with

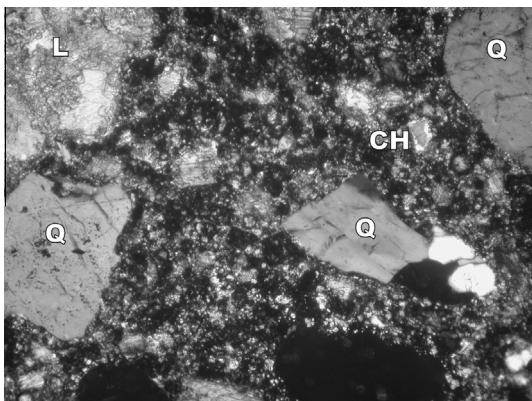


Fig. 7. Thin section micrograph (TSM) of C1 control sample. Horizontal field of view = 0.7 mm.

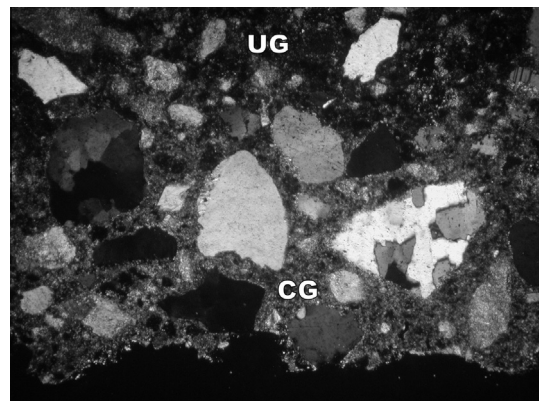


Fig. 9. Thin section micrograph (TSM) of C7-28 scCO₂-treated sample. Horizontal field of view = 1.4 mm.

CO₂ – and the strength of the samples. For example, in the C7 and/or C7-28 samples (compared to those remaining uncured prior to SCC treatment), XRD and TG indicated that CH and residual C₃S were minimally depleted by SCC; DTA/TG indicated that the effect of SCC on the gel phase was minimal; pycnometry recorded only a small drop in porosity owing to SCC treatment; and petrographic images clearly show that the so-called ‘carbonation front’ has penetrated only ~0.5 mm into the sample. Yet the strength developed in these apparently minimally carbonated samples was similar to that developed in fully-carbonated samples.

The strength-bearing phase in a cement composite matrix is the C–S–H gel, whether in a ‘pure’ cement-binder system, one modified with lime (as studied here), and/or modified with siliceous additions; thus it is understandable that depletion of crystalline phases is not coupled to strength increases. However, DTA and petrography of minimally-carbonated samples both suggest that the C–S–H is not significantly altered chemically (i.e., fully decalcified) or morphologically by SCC treatment; or, put another way, the subtle changes in C–S–H microstructure responsible for the strength increase are not detectable by these methods. Previous work by Short et al. [15] using NMR suggested that SCC treatment can fundamentally change the nature of the silica polymerisation in C–S–H gel and this may well be the effect that is at work here. The changes are clearly fundamental (i.e. associated with intrinsic physico-chemical changes in the matrix), as the strength is increased independently of the porosity. This is interesting since many literatures [3–8,18,19] explain the enhancement in strength of carbonated cementitious matrices purely by reduction of porosity through formation of C₂S crystals and their precipitation in the matrix pores; clearly this is not the case in this instance. Furthermore, the C–S–H phase must be much more susceptible to SCC carbonation than the crystalline phases. The very thin carbonated layer seen in Fig. 9 is insufficient to account for the increase in strength in these samples, implying that in fact scCO₂ has diffused much more deeply into the sample and partially reacted with the C–S–H in the bulk of the matrix relatively quickly. The surface reaction with CH (and, to a lesser extent, unhydrated cement) has proceeded much more slowly and indeed may have been self-limiting via the formation of a protective layer. Clearly, the traditional notion that a carbonation front proceeds in an orderly fashion through a cement-based calcareous composite sample during SCC is deficient. This may also have implications for the study of environmental carbonation.

References

- [1] Jones R. Supercritical CO₂ carbonation of cement and cement-fiber composites: the Supramics process. In: Anastas P, Williamson TC, Heine L, editors. *Green Engineering*. Washington, DC: American Chemical Society; 2001. p. 124–35.
- [2] Jones RH. Cement treated with high pressure CO₂. US patent 5518540, 21 May 1996.
- [3] Onan DD. Effects of supercritical carbon dioxide on well cements. In: Society of Petroleum Engineers of AIME, editor. *Proceeding of the Permian Basin Oil and Gas Recovery Conference*. Midland, TX, USA; 1984. p. 161–72.
- [4] St Jones DA, Poole AW, Sims I. *Concrete petrography: a handbook of investigative techniques*. London: Arnold; 1998.
- [5] Seatta V, Nenhard BA, Scherefler A, Vitaliani RV. The carbonation of concrete and the mechanism of moisture, heat and carbon dioxide flow through porous materials. *Cem Concr Res* 1993;23(4):761–72.
- [6] Fernandez Bertos M, Simons SJR, Hills CD, Carey PJ. A review of accelerated technology in the treatment of cement based materials and sequestration of CO₂. *J Hazard Mater* 2004;112(3):193–205.
- [7] Garcia-Gonzalez CA, Hidalgo A, Andrade C, Alonso MC, Fraile J, Lopez-Periago AM, et al. Modification of composition and microstructure of Portland cement pastes as a result of natural and supercritical carbonate procedures. *Ind Eng Chem Res* 2006;45(14):4985–92.
- [8] Garcia-Gonzalez CA, Hidalgo A, Fraile J, Lopez-Periago AM, Andrade C, Domingo C. Porosity and water permeability study of supercritical carbonated cement pastes involving mineral additions. *Ind Eng Chem Res* 2007;46(8):2488–96.
- [9] Neville AM. *Properties of concrete*. New York: John Wiley & Sons; 1996.
- [10] Johannesson B, Utgenannt P. Microstructural changes by carbonation of cement mortars. *Cem Concr Res* 2001;31(6):925–31.
- [11] Short NR, Purnell P, Page CL. Preliminary investigations into the supercritical carbonation of cement pastes. *J Mater Sci* 2001;36(1):35–41.
- [12] Purnell P, Short NR, Page CL. Super-critical carbonation of glass fibre reinforced cement Part 1: Mechanical testing and chemical analysis. *Composites: Part A* 2001;32(12):1777–87.
- [13] Purnell P, Seneviratne AMG, Short NR, Page CL. Super-critical carbonation of glass fibre reinforced cement Part 2: Microstructural observation. *Composites: Part A* 2003;34(11):1105–12.
- [14] Seneviratne AMG, Short NR, Purnell P, Page CL. Preliminary investigations of the dimensional stability of supercritically carbonated glass fibre reinforced cement. *Cem Concr Res* 2002;32(10):1639–44.
- [15] Short NR, Brough AR, Seneviratne AMG, Purnell P, Page CL. Preliminary investigations of the phase composition and fine pore structure of supercritically carbonated cement paste. *J Mater Sci* 2004;39(18):5683–7.
- [16] Lawrence RM, Mays TJ, Rigby SP, Walker P, D'Ayala D. Effect of carbonation on the pore structure of non-hydraulic lime mortars. *Cem Concr Res* 2007;37(7):1059–69.
- [17] Arandigoyen M, Bicer-Simsir B, Alvarez JI, Lange DA. Variation of microstructure with carbonation in lime and blended pastes. *Appl Surf Sci* 2005;252(20):7562–71.
- [18] Lang LC, Hills CD, Poole AB. The effect of accelerated carbonation on the properties of cement solidified waste forms. *Waste Manage* 1996;16(8):757–63.
- [19] Knopf FC, Roy A, Samrow HA, Dooley KM. High pressure moulding and carbonation of cementitious materials. *Ind Eng Chem Res* 1999;38(7):2641–9.
- [20] Van Gerven T, Van Baelen D, Dutre V, Vandecasteele C. Influence of carbonation and carbonation methods on leaching of metal mortars. *Cem Concr Res* 2004;34(1):149–56.
- [21] Purnell P, Farahi E, Short NR. Supercritical carbonation of lime based sustainable structural ceramics. *Adv Appl Ceram* 2010;109(5):280–6.
- [22] Farahi E, Purnell P, Short NR. Supercritical carbonation of calcareous composite: influence of mix design. *Cem Concr Compos* 2013.
- [23] Farahi E. Advanced calcareous ceramics via novel green processing and supercritical carbonation. PhD thesis, Warwick, University of Warwick; 2009.
- [24] Farahi E, Purnell P, Short NR. Advanced calcareous ceramics via novel green processing and supercritical carbonation. In: *Proceeding of International conference on Sustainable construction materials and technologies*, Coventry-UK; June 11–13, 2007. p. 359–66.
- [25] Ramachandran VS. *Applications of differential thermal analysis in cement chemistry*. New York: Chemical Publishing Co.; 1969.
- [26] Aligizaki KK. *Pore structure of cement based materials; testing, interpretation and requirement*. London: Taylor and Francis; 2006.